



A Journal of the Gesellschaft Deutscher Chemiker

Angewandte Chemie

GDCh

International Edition

www.angewandte.org

Accepted Article

Title: Single-Molecule Imaging of Active Mitochondrial Nitroreductases using a Photo-Crosslinking Fluorescent Sensor

Authors: Zacharias Thiel and Pablo Rivera-Fuentes

This manuscript has been accepted after peer review and appears as an Accepted Article online prior to editing, proofing, and formal publication of the final Version of Record (VoR). This work is currently citable by using the Digital Object Identifier (DOI) given below. The VoR will be published online in Early View as soon as possible and may be different to this Accepted Article as a result of editing. Readers should obtain the VoR from the journal website shown below when it is published to ensure accuracy of information. The authors are responsible for the content of this Accepted Article.

To be cited as: *Angew. Chem. Int. Ed.* 10.1002/anie.201904700
Angew. Chem. 10.1002/ange.201904700

Link to VoR: <http://dx.doi.org/10.1002/anie.201904700>
<http://dx.doi.org/10.1002/ange.201904700>



COMMUNICATION

Single-Molecule Imaging of Active Mitochondrial Nitroreductases using a Photo-Crosslinking Fluorescent Sensor

Zacharias Thiel and Pablo Rivera-Fuentes*

Abstract: Many biomacromolecules are known to cluster in microdomains with specific subcellular localization. In the case of enzymes, this clustering greatly defines their biological functions. Nitroreductases are enzymes capable of reducing nitro groups to amines, and play a role in detoxification and pro-drug activation. Although nitroreductase activity has been detected in mammalian cells, the subcellular localization of this activity remains incompletely characterized. Here, we report a fluorescent probe that enables super-resolved imaging of pools of nitroreductase activity within mitochondria. This probe is activated sequentially by nitroreductases and light to give a photo-crosslinked adduct of active enzymes. In combination with a general photoactivatable marker of mitochondria, we performed two-color, three-dimensional, single-molecule localization microscopy. These experiments allowed us to image the sub-mitochondrial organization of microdomains of nitroreductase activity.

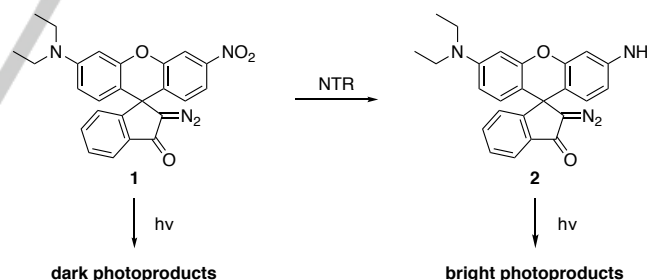
Fluorescence microscopy has become an indispensable tool for the study of intracellular localization and dynamics of enzymatic activity in living systems. Small-molecule fluorogenic probes for enzymatic activity usually consist of fluorescent dyes functionalized with groups that resemble the substrates of the enzyme and quench the fluorescence. Emission is restored upon enzymatic conversion of these functional groups, revealing the presence of active enzymes.^[1,2] A commonly overlooked problem of these turn-on probes is the rapid diffusion of the fluorophores following enzymatic activation and the potential accumulation at intracellular locations that differ from the origin of activation. Hence, mapping the real subcellular distribution of enzymatic activity can be challenging and results can easily be misinterpreted. A possible way to minimize the unwanted diffusion of activated fluorophores and increasing the precision of localization of enzymatic activation is achieved by targeting the probe to certain organelles.^[3–5] This strategy, however, assumes certain intracellular localization and enzymes that are active in other organelles might be neglected.

Another constraint of current fluorogenic probes is resolution, which is limited by diffraction of light. Even though super-resolution microscopy techniques such as stochastic optical reconstruction microscopy (STORM)^[6] and photoactivation localization microscopy (PALM)^[7] are well established, there is a lack of fluorescent sensors that are specifically optimized for these techniques. We recently developed a sensing mechanism that is compatible with STORM.^[8] We reported that photoactivatable diazoindanone-modified xanthenes bearing electron withdrawing substituents mainly form non-fluorescent photoproducts upon irradiation. Irradiation following

enzymatic transformation of the substituent into an electron-donating group yields highly fluorescent photoproducts that display minimal diffusion.^[8]

Herein, we apply this principle to develop a probe for the detection of nitroreductase activity in mammalian cells. Nitroreductases (NTRs) are a class of enzymes that catalyze the reduction of nitroaromatic compounds to their corresponding anilines.^[9,10] NTRs are categorized into oxygen insensitive (Type I) and oxygen sensitive (Type II). These enzymes reduce nitro groups via an initial two electron or one electron step, respectively. The presence of Type II NTRs in tumors under hypoxic conditions is well established, and there are many fluorogenic methods for the detection of solid tumors based on this enzymatic activity.^[11,12] Recently, probes were reported to detect mitochondrial NTR activity even under normoxic conditions, indicating the presence of Type I NTRs.^[13] The role of NTRs in mammalian cells, however, remains unclear and their subcellular distribution is incompletely characterized. Some sources even report complete absence of NTR activity in non-cancerous cells.^[14]

To characterize the subcellular distribution of NTR activity with nanometric precision, we designed photoactivatable probe **1** (Scheme 1). We envisioned that the nitro group of this diazoindanone-modified rhodamine analog would withdraw enough electron density to give mainly non-fluorescent products upon photoirradiation. Enzymatic conversion by NTRs, however, would produce the amino-substituted electron-rich xanthenes derivative **2** (Scheme 1), which would yield a fluorescent product upon irradiation.



Scheme 1. Proposed mechanism for detecting NTR activity using photoactivatable probe **1**. NTR = nitroreductase.

We first tested the photochemistry of the probe before and after conversion of the nitro group, for which we prepared compounds **1** and **2** (Scheme S1 and S2). Solutions of **1** and **2** (10 μM in phosphate buffered saline (PBS), pH = 7.4/acetoneitrile 1:1) did not display strong absorption in the visible range or any fluorescence (Figures S1 and S2). These solutions were exposed to 350 nm light (8 lamps of 8 W each) for 15 min (Figure 1A and 1B). After irradiation, the solution of compound **1** did not display any measurable change in fluorescence (Figures 1B and S3), whereas a significant increase was observed when compound **2** was irradiated. The absorption and emission spectra of the irradiated solutions of compound **2** further confirmed the appearance of a prominent absorption band at 532 nm and a

[*] Z. Thiel, Prof. Dr. P. Rivera-Fuentes
Laboratorium für Organische Chemie, ETH Zürich, HCI G329
Vladimir-Prelog-Weg 3, 8093 Zürich (Switzerland)
Email: pablo.rivera-fuentes@org.chem.ethz.ch

Supporting information for this article is given via a link at the end of the document.

COMMUNICATION

fluorescence emission band at 550 nm (Figures 1B and S4). These features suggest the formation of an emissive xanthene photoproduct. To confirm the identity of the putative photoproduct, we prepared compound **3** (Figure 1C), which we expected to be the major photoproduct.^[8,15,16] Liquid chromatography coupled with mass spectrometry (LC-MS) confirmed that compound **3** is indeed the major photoproduct formed upon irradiation of **2** in water (Figure S5). The same results were obtained when compound **2** was irradiated with 405 nm light, which is commonly used in fluorescence microscopy (Figure S6). Irradiation of **1**, however, produced a variety of unidentified non-fluorescent photoproducts (Figure S5) as indicated by the chromatogram of its irradiated solution. The photophysical properties and quantum yields of photoconversion are summarized in Table S1 and Figures S7 and S8. These data confirm that the formation of fluorescent photoproducts is strongly suppressed by the presence of the electron withdrawing nitro group.

Next, we tested the applicability of compound **1** as a probe for the detection of NTR activity in cuvettes using purified NTR from *E. coli* (NfsB, Figure 1D). A solution of **1** (10 μM in PBS, containing 500 μM NADH) was incubated with NTR (10 $\mu\text{g mL}^{-1}$) for 30 min and the fluorescence was determined before and after irradiation with 350 nm for 15 min. In presence of NTR, irradiation induces a significant increase in fluorescence. To exclude the possibility of the observed fluorescence increase arising from non-specific interactions with proteins,^[17] **1** was treated with NTR in the absence of the cofactor NADH and with bovine serum albumin (10 $\mu\text{g mL}^{-1}$) prior to irradiation. No increase in fluorescence was detected in either case (Figure 1D). We also verified that the photoactivation outcome does not depend on the pH of the medium (Figure S9). The lack of fluorescence increase in absence of active NTR indicates that enzymatic transformation of **1** to **2** prior to photoactivation is necessary for fluorescence signal. The formation of **2** upon treatment of **1** with NTR was further observed by LC-MS experiments (Figure S10).

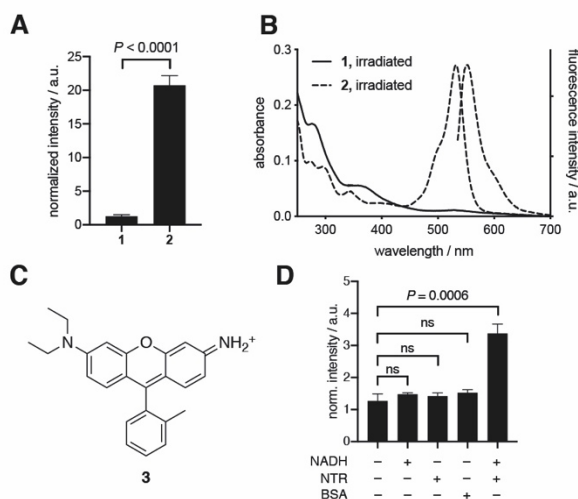


Figure 1. A) Fluorescence increase upon photoactivation of solutions of **1** and **2** in phosphate buffered saline pH = 7.4/acetonitrile 1:1. B) Absorbance and fluorescence emission spectra of irradiated ($\lambda = 350$ nm) solutions of **1** and **2**. C) Structure of the main fluorescent photoproduct formed by photolysis of **2**. D) Photoactivation of probe **1** in the presence of bacterial NTR, with and without the co-factor NADH, or only in the presence of BSA. In all cases bars are averages of independent measurements ($N = 3$) and error bars represent standard deviation. BSA = bovine serum albumin, ns: $P > 0.05$, NTR = nitroreductase.

Having confirmed the reactivity of compound **1** towards NTR, we evaluated its performance as a probe for NTR activity in live human embryonic kidney (HEK 293) cells using confocal fluorescence microscopy. Cells were incubated with compound **1** at a concentration of 10 μM for 10 min and subsequently exposed to 405 nm light (~ 80 mW, 10 s). Photoactivation led to a substantial increase in fluorescence signal (Figure 2A and 2B). Notably, this increase in photoactivation is significantly lower in cells pretreated with dicoumarol, a known inhibitor of bacterial NTR (Figure S11).^[18] Colocalization analysis using various genetically encoded organelle markers revealed that the signal obtained after photoactivation predominantly occurred in mitochondria (Figure 2C and S12), which agrees with previously reported targeted fluorescence reporters for NTR activity.^[13] Cells that were treated with **2** did not display signal that is specifically localized to mitochondria, indicating that the localization arises from enzymatic transformation of **1** in mitochondria rather than accumulation of **2** after enzymatic reaction (Figure S13).

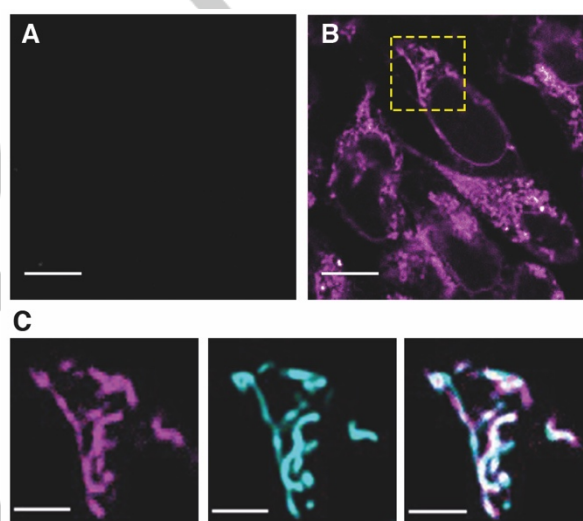


Figure 2 A) Live HEK 293 cells imaged with 561 nm excitation light after incubation with **1** (10 μM) for 10 min before photoactivation. B) Same cells as displayed in panel A imaged at 561 nm excitation light after exposure to 405 nm light (~ 80 mW, 10 s). C) Region of interest indicated with a yellow, dotted square in panel B. Imaged at 561 nm (photoactivated probe **1**, left), at 445 nm (mTurquoise2-COX8A, mitochondrial marker, center), and overlay of the photoactivated probe **1** and mitochondrial marker (right). Scale bars: 5 μm (panels A and B) and 2 μm (panels C).

The localization of enzymatic activity can be mistakenly assigned if the fluorogenic probe diffuses freely after enzymatic activation. Based on the mechanism of photoactivation of diazoindanones, we reasoned that the ketene intermediate that is formed during the photoinduced Wolff-rearrangement^[16] could be readily trapped by nucleophilic side chains of proteins in its vicinity (Figure 3A). In order to validate this hypothesis, we investigated the propensity of **2** to form covalent adducts with amino acids upon irradiation in a cell-free environment. We irradiated **2** (100 μM in acetonitrile) in the presence of *N*-protected amino acids (5 mM). LC-MS analysis indicated that after 15 min of irradiation, compound **2** formed adducts with several amino acids bearing nucleophilic side chains, including cysteine, tyrosine, lysine, and histidine (Figure S14). Notably, when irradiated in aqueous solution, the reaction with amino



COMMUNICATION

acids was not observed because water is a competitive nucleophile that is present in large excess (Figure S14). Therefore, the ketene intermediate of compound **2** (Figure 3A) can only be trapped by nucleophiles that are present in close proximity immediately after photoactivation. We hypothesized that if the photochemical reaction occurs immediately after enzymatic conversion, the nitroreductase itself might be able to trap the ketene. To test this hypothesis, NTR from *E. coli* was incubated with **1** and immediately irradiated with 405 nm light. After purification by gel electrophoresis, the band corresponding to NTR displays fluorescence at 602 ± 50 nm, whereas a non-irradiated control sample remains completely non-fluorescent. These data confirm that photoactivation immediately after the enzymatic transformation of **1** to **2** results in covalent modification of the activating enzyme with a fluorescent label. This approach to label enzymes was further tested in live HEK 293 cells that were incubated with **1** and exposed to 350 nm light (8 lamps of 8 W each). Gel electrophoresis of lysates revealed a few distinct fluorescent bands indicating enzymes with potential nitroreductase activity (Figure S15).

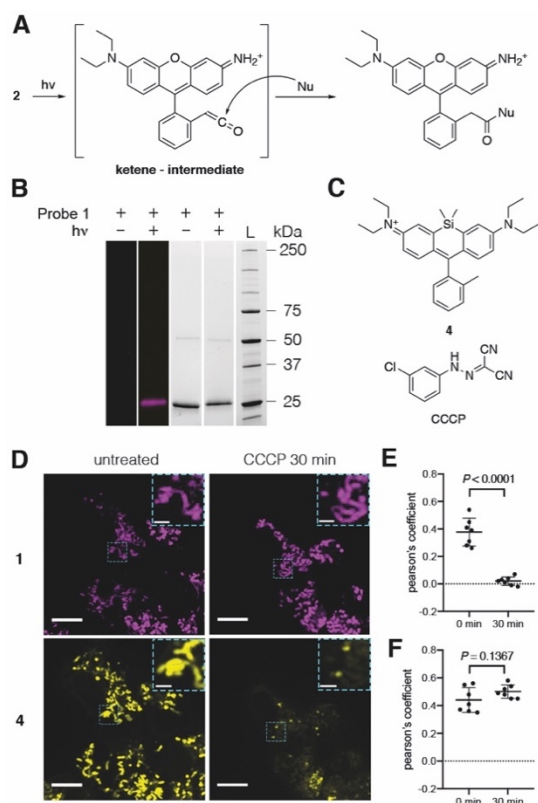


Figure 3. A) Proposed mechanism of photolysis of compound **2**, ketene formation and nucleophilic attack. B) Sodium dodecyl sulfate – polyacrylamide gel electrophoresis of NTR from *E. coli* crosslinked with fluorophores imaged at 602 ± 50 nm (dark lanes) and as stain-free gel image (white lanes). C) Structures of compound **4** and CCCP. D) Fluorescence images of live HEK 293 cells treated with compound **1** (10 μ M, 10 min) imaged with 515 nm excitation light (magenta) and compound **4** (0.1 μ M, 30 min) imaged with 640 nm excitation light (yellow) after exposure to 405 nm light (~80 mW, 10 s) before and 30 min after addition of CCCP (20 μ M). Selected ROIs (dotted cyan squares) are displayed enlarged as insets. E) Colocalization between the signals obtained from compounds **1** and **4** in untreated cells before and 30 min after addition of CCCP (20 μ M). F) Colocalization between the signals obtained from compounds **1** and **4** in control cells without addition of CCCP over a course of 30 min. Scale bars: 5 μ m (panel D, insets: 1 μ m). Graphs display individual values, averages, and standard deviations for $N = 7$ independent measurements from three biological replicates. Nu = nucleophile.

Although the probe is able to label the nitroreductases covalently, many molecules might still escape the proximity of the protein, react with water, and become a diffusible small molecule (Figure 3A). We noticed, however, that this small molecule has a very low quantum yield of emission in water. In contrast, the quantum yield of emission in apolar solvents is much higher (Figure S16). This fluorogenicity provides additional contrast for specific imaging of fluorophores covalently linked to proteins that provide an apolar environment.^[19,20]

Encouraged by these results, we tested whether this covalent labeling also occurs in nitroreductases in live HEK 293 cells. We used 405 nm light to irradiate a small region of interest (ROI) within a cell that had been incubated with **1** and observed the diffusion of fluorescent molecules over a course of 10 min (Figure S17). Analysis of the signal revealed that the fluorescence stayed within the ROI, indicating minimal diffusion of the fluorophores formed by photoactivation of **2** within the cell. Lipophilic organic molecules carrying a permanent positive charge are known to be taken up and retained by mitochondria.^[21,22] The fluorophore generated by photolysis of **2** carries a permanent positive charge, which makes it amenable for uptake and retention in mitochondria without covalent labeling. To exclude this possibility, we used the protonophore carbonyl cyanide *m*-chlorophenyl hydrazine (CCCP) to depolarize mitochondria, which induces dissipation of positively charged species.^[23] Cells pretreated with **1** and the cationic dye **4**, which also localizes to mitochondria (Figure S18), were exposed to 405 nm light. Fluorescence images taken at 515 nm and 640 nm revealed that the signals of the two fluorophores colocalize with each other and with mitochondria (Figure 3D). Whereas addition of CCCP (20 μ M) induced dissipation of compound **4** after 30 min, photoactivated compound **1** remained in mitochondria, resulting in a drastic decrease in the colocalization between compounds **1** and **4** (Figure 3E). Mitochondria of cells that were not treated with CCCP retained both compounds equally, resulting in no change in colocalization (Figure 3F). These data, together with the results of the previous experiments, confirm that **1** can be used to covalently label proteins in cells upon irradiation.

Photoactivatable probes that label proteins selectively are ideally suited for single-molecule localization microscopies such as STORM. Employing probe **1**, we set out to map the distribution of active nitroreductases within the mitochondria of live HEK 293 cells. In order to label mitochondria evenly and non-specifically, we prepared compound **5** (Figure 4A), a mitochondria-targeting,^[24] far-red-emitting photoactivatable probe (Figure S19).^[17] Using this compound and probe **1**, we performed two-color, three-dimensional STORM imaging. To minimize diffusion of compound **1** after enzymatic conversion and obtain super-imposable signals of the two imaging channels, we applied a 405 nm photoactivation pulse (100 μ s), followed by 40 alternating readout frames with 514 nm (50 ms) and 647 nm excitation (50 ms), respectively. This sequence was repeated every 4 s. From this acquisition, a super-resolved image of mitochondria as well as a super-resolved image of nitroreductase activity were reconstructed (Figure 4B) with average localization precisions of 40 ± 17 nm and 63 ± 18 nm, respectively. It must be mentioned that typical STORM experiments usually achieve better localization precisions (<20 nm), but most of these experiments employ fixed cells and do not report on the activity of the enzyme. In this case, imaging enzymatic activity requires live-cell STORM imaging and the localization precision in these experiments is

COMMUNICATION

generally eroded by motion blur. Nevertheless, our super-resolved images are able to distinguish domains of nitroreductase activity to a greater extent than diffraction-limited methods (Figure 4B).

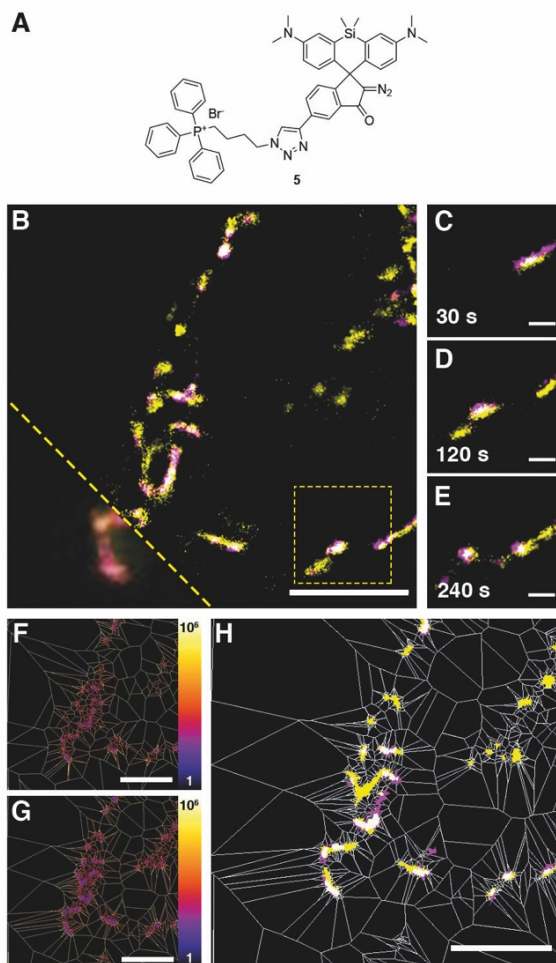


Figure 4. STORM super-resolution microscopy of nitroreductase activity in live HEK 293 cells. A) Structure of compound **5** used to label mitochondria evenly. B) Super-resolved image, reconstructed from 200 frames (20 s) of a cell treated with compound **1** (15 μM) in magenta and compound **5** (1 μM) in yellow. The image is displayed as a z-projection of the signals collected from a total depth of 1.6 μm . The diffraction limited counterpart is marked with the dashed yellow line in the lower left corner. C – D) Magnifications of the region outlined by the yellow rectangle in panel B at various time points. Each image was reconstructed from 100 frames (10 s). F) Voronoi tessellation of the signals obtained from compound **1** of the image displayed in panel B. G) Voronoi tessellation of the signals obtained from compound **5** of the image displayed in panel B. Polygons are colored according to their areas, see color bar (units: nm^2). H) Overlay of the identified clusters using the signals from compound **1** (magenta) and compound **5** (yellow). Scale bars = 5 μm (panels B, F, G, and H), 1 μm (panels C, D, and E).

These data revealed that nitroreductase activity occurs predominantly in mitochondria. This colocalization can be observed throughout the entire duration of image acquisition, even in moving mitochondria (Figure 4C – 4E). The enzymatic activity, however, does not appear to be evenly distributed within mitochondria but rather seems to cluster in certain regions. We used Voronoi tessellation^[25]

to identify clusters of active nitroreductases (Figure 4F and 4G) based on single-molecule signals. First, regions corresponding to mitochondria were identified using the signals generated by compound **5** (yellow regions in Figure 4H). Analysis of the signals generated by compound **1** (magenta regions in Figure 4H), gave clusters that overlap with the previously identified regions corresponding to mitochondria (white regions in Figure 4H). From these data, we conclude that nitroreductase activity is indeed mainly located within mitochondria, but it is not evenly distributed within these organelles. This experiment therefore reveals that mitochondrial nitroreductases cluster in domains of increased activity, and probe **1** is able to image these domains beyond the limit of diffraction of light.

In summary, we developed a probe that is activated by nitroreductases and generates a fluorescent photoproduct upon photoactivation. Furthermore, the probe covalently binds to nucleophilic residues of proteins and does not diffuse freely during image acquisition. Using this photo-crosslinking, fluorogenic probe, we demonstrated that nitroreductase activity is observed in microdomains within mitochondria. It is not clear yet which enzymes display nitroreductase activity in mammalian mitochondria, but ongoing work in our lab is aimed at identifying them.

Acknowledgements

This work was supported by ETH Zurich. We thank Alina Tirla for the preparation of compound **4**, Dr. Nils Trapp for X-ray crystallography, and Dr. Dorothea Pinotsi for useful discussions.

Conflict of interest

The authors declare no conflicts of interest.

Keywords: fluorescent probes • super-resolution microscopy • photo-crosslinking • nitroreductases • photoactivation

- [1] J. B. Grimm, L. M. Heckman, L. D. Lavis, *Prog. Mol. Biol. Transl. Sci.* **2013**, *113*, 1–34.
- [2] W. Chyan, R. T. Raines, *ACS Chem. Biol.* **2018**, *13*, 1810–1823.
- [3] B. Huang, W. Chen, Y.-Q. Kuang, W. Liu, X.-J. Liu, L.-J. Tang, J.-H. Jiang, *Org. Biol. Chem.* **2017**, *15*, 4383–4389.
- [4] R. S. Kathayat, P. D. Elvira, M. Z. Springer, L. E. Drake, *Nat. Commun.* **2018**, *9*, 334.
- [5] M. N. Levine, T. T. Hoang, R. T. Raines, *Chem. Biol.* **2013**, *20*, 614–618.
- [6] M. J. Rust, M. Bates, X. Zhuang, *Nat. Methods* **2006**, *3*, 793–795.
- [7] E. Betzig, G. H. Patterson, R. Sougrat, O. W. Lindwasser, S. Olenych, J. S. Bonifacino, M. W. Davidson, J. Lippincott-Schwartz, H. F. Hess, *Science* **2006**, *313*, 1642–1645.
- [8] E. A. Halabi, Z. Thiel, N. Trapp, D. Pinotsi, P. Rivera-Fuentes, *J. Am. Chem. Soc.* **2017**, *139*, 13200–13207.
- [9] I. Oliveira, D. Bonatto, J. Antonio, P. Henriques, *Curr. Res., Technol. Ed. Top. Appl. Microbiol. Microb. Biotechnol.* **2010**, 1008–1019.
- [10] M. D. Roldán, E. Pérez-Reinado, F. Castillo, C. Moreno-Vivián, *FEMS Microbiol Rev* **2008**, *32*, 474–500.

COMMUNICATION

- [11] L. Cui, Y. Zhong, W. Zhu, Y. Xu, Q. Du, X. Wang, X. Qian, Y. Xiao, *Org. Lett.* **2011**, *13*, 928–931.
- [12] C. Xue, Y. Lei, S. Zhang, Y. Sha, *Anal. Methods* **2015**, *7*, 10125–10128.
- [13] A. Chevalier, Y. Zhang, O. M. Khmour, J. B. Kaye, S. M. Hecht, *J. Am. Chem. Soc.* **2016**, *138*, 12009–12012.
- [14] T. D. Gruber, C. Krishnamurthy, J. B. Grimm, M. R. Tadross, L. M. Wysocki, Z. J. Gartner, L. D. Lavis, *ACS Chem. Biol.* **2018**, *13*, 2888–2896.
- [15] V. N. Belov, G. Y. Mitronova, M. L. Bossi, V. P. Boyarskiy, E. Hebisch, C. Geisler, K. Kolmakov, C. A. Wurm, K. I. Willig, S. W. Hell, *Chem. Eur. J.* **2014**, *20*, 13162–13173.
- [16] V. N. Belov, C. A. Wurm, V. P. Boyarskiy, S. Jakobs, S. W. Hell, *Angew. Chem. Int. Ed.* **2010**, *49*, 3520–3523; *Angew. Chem.* **2010**, *122*, 3598–3602.
- [17] J. B. Grimm, B. P. English, H. Choi, A. K. Muthusamy, B. P. Mehl, P. Dong, T. A. Brown, J. Lippincott-Schwartz, Z. Liu, T. Lionnet, L. D. Lavis, *Nat. Methods* **2016**, *13*, 985–988.
- [18] R. L. Koder, A.-F. Miller, *Biochim. Biophys. Acta, Protein Struct. Mol. Enzym.* **1998**, *1387*, 395–405.
- [19] B. E. Cohen, A. Pralle, X. Yao, G. Swaminath, C. S. Gandhi, Y. N. Jan, B. K. Kobilka, E. Y. Isacoff, L. Y. Jan, *Proc. Natl. Acad. Sci. U.S.A.* **2005**, *102*, 965–970.
- [20] B. E. Cohen, T. B. McAnaney, E. S. Park, Y. N. Jan, S. G. Boxer, L. Y. Jan, *Science* **2002**, *296*, 1700–1703.
- [21] R. W. Horobin, S. Trapp, V. Weissig, *J. Control. Release* **2007**, *121*, 125–136.
- [22] S. Rin Jean, D. V. Tulumello, S. P. Wisnovsky, E. K. Lei, M. P. Pereira, S. O. Kelley, *ACS Chem. Biol.* **2014**, *9*, 323–333.
- [23] R. C. Scaduto, L. W. Grotyohann, *Biophys. J.* **1999**, *76*, 469–477.
- [24] J. Zielonka, J. Joseph, A. Sikora, M. Hardy, O. Ouari, J. Vasquez-Vivar, G. Cheng, M. Lopez, B. Kalyanaraman, *Chem. Rev.* **2017**, *117*, 10043–10120.
- [25] F. Levet, E. Hosy, A. Kechkar, C. Butler, A. Beghin, D. Choquet, J.-B. Sibarita, *Nat. Methods* **2015**, *12*, 1065–1071.

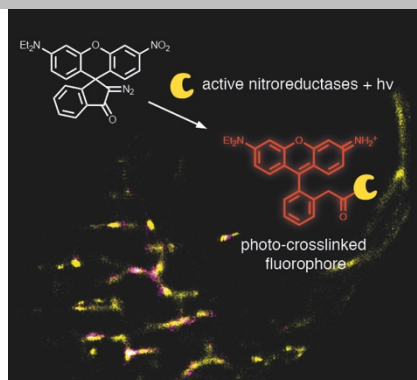
COMMUNICATION

Entry for the Table of Contents

Layout 1:

COMMUNICATION

A fluorogenic, activity-based, photo-crosslinking probe is used to map the sub-mitochondrial distribution of mammalian nitroreductases.



Zacharias Thiel and Pablo Rivera-Fuentes*

Page No. – Page No.

Single-Molecule Imaging of Active Mitochondrial Nitroreductases using a Photo-Crosslinking Fluorescent Sensor